# Lab on a Chip

Accepted Manuscript

This is an *Accepted Manuscript*, which has been through the Royal Society of Chemistry peer review process and has been accepted for publication.

Accepted Manuscripts are published online shortly after acceptance, before technical editing, formatting and proof reading. Using this free service, authors can make their results available to the community, in citable form, before we publish the edited article. We will replace this *Accepted Manuscript* with the edited and formatted *Advance Article* as soon as it is available.

You can find more information about *Accepted Manuscripts* in the **Information for Authors**.

Please note that technical editing may introduce minor changes to the text and/or graphics, which may alter content. The journal's standard **Terms & Conditions** and the **Ethical guidelines** still apply. In no event shall the Royal Society of Chemistry be held responsible for any errors or omissions in this *Accepted Manuscript* or any consequences arising from the use of any information it contains.

Table of Contents Figure:
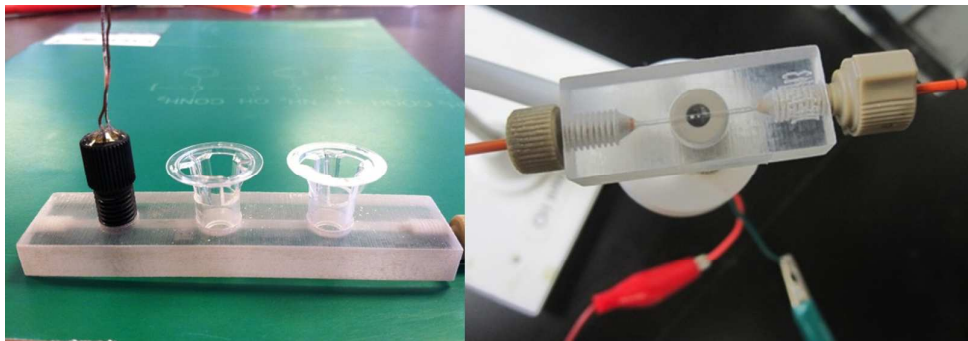
1   **Title**

2   3D Printed Microfluidic Devices with Integrated Versatile and Reusable Electrodes

3

4   **Authors**

5   Jayda L. Erkal,[a] Asmira Selimovic,[b] Bethany C. Gross,[a] Sarah Y. Lockwood,[a] Eric L. Walton,[a]

6   Stephen McNamara,[a] R. Scott Martin,[b] and Dana M. Spence[a],*

7

8   [a] Department of Chemistry, Michigan State University, 578 S. Shaw Lane, East Lansing, MI

9   48824

10   [b] Department of Chemistry, Saint Louis University, 3501 Laclede Ave, St. Louis, MO 63103

11

12   **Corresponding Author Information:**

13   Dana M. Spence

14   578 S. Shaw Lane

15   East Lansing, MI 48824

16   Phone: 517-355-9715 ext.174

17   Email: dspence@chemistry.msu.edu

18

19

20

21

22

23

24 **TOC Entry**

25 We present two 3D printed fluidic devices capable of 1) flow-based electrochemical

26 determination of dopamine and nitric oxide and 2) electrochemical measurement of

27 oxygen while simultaneously collecting secreted molecules from red blood cells exposed to

28 varying oxygen tensions.

29

30 **Abstract**

31 We report two 3D printed devices that can be used for electrochemical detection. In both

32 cases, the electrode is housed in commercially available, polymer-based fittings so that the

33 various electrode materials (platinum, platinum black, carbon, gold, silver) can be easily

34 added to a threaded receiving port printed on the device; this enables a module-like

35 approach to the experimental design, where the electrodes are removable and can be easily

36 repolished for reuse after exposure to biological samples. The first printed device

37 represents a microfluidic platform with a 500 x 500 μm channel and a threaded receiving

38 port to allow integration of either polyetheretherketone (PEEK) nut-encased glassy carbon

39 or platinum black (Pt-black) electrodes for dopamine and nitric oxide (NO) detection,

40 respectively. The embedded 1 mm glassy carbon electrode had a limit of detection (LOD) of

41 500 nM for dopamine and a linear response (R^2= 0.99) for concentrations between 25-500

42 μM. When the glassy carbon electrode was coated with 0.05% Nafion, significant exclusion

43 of nitrite was observed when compared to signal obtained from equimolar injections of

44 dopamine. When using flow injection analysis with a Pt/Pt-black electrode and standards

45 derived from NO gas, a linear correlation (R^2 = 0.99) over a wide range of concentrations

46 (7.6 - 190 μM) was obtained, with the LOD for NO being 1 μM. The second application

47   showcases a 3D printed fluidic device that allows collection of the biologically relevant

48   analyte adenosine triphosphate (ATP) while simultaneously measuring the release

49   stimulus (reduced oxygen concentration). The hypoxic sample (4.76 $\pm$ 0.53 ppm oxygen)

50   released 2.37 $\pm$ 0.37 times more ATP than the normoxic sample (8.22 $\pm$ 0.60 ppm oxygen).

51   Importantly, the results reported here verify the reproducible and transferable nature of

52   using 3D printing as a fabrication technique, as devices and electrodes were moved

53   between labs multiple times during completion of the study.

54

Introduction

56   Electrodes have been successfully integrated with traditional polymer-based and glass-

57   based microfluidic devices since the early 2000s.[1, 2] Polydimethylsiloxane (PDMS) – based

58   devices, either composed of all PDMS or PDMS-glass hybrids, are popular for integrating

59   electrochemical detection in the microchip format due to its ease of fabrication and the

60   ability of PDMS to seal (either reversibly or irreversibly) over the electrode of interest. A

61   wide variety of techniques have been used to incorporate electrodes into these types of

62   PDMS microfluidic devices including insertion of traditional wires/electrodes into the

63   device,[3, 4] and use of screen-printed carbon ink electrodes,[5, 6] with the most popular method

64   being fabrication of electrodes by sputtering/evaporation and photolithography.[7-11] Much

65   of this early work drove development in electrophoresis-based detection of biologically

66   relevant analytes such as catecholamines. While these devices have been used for a wide

67   variety of applications including cellular analysis,[12] the utility of soft polymer devices

68   suffers ultimately because of their lack of reusability. Irreversibly-sealed devices cannot be

69   reused when a portion of the device fails. With reversibly sealed devices, most of the

70   approaches to date do not permit the electrode to be repolished or regenerated for

71   replicate experiments if the electrode is compromised. Biological studies typically require

72   replicate experiments from multiple samples/subjects, so device-to-device (or electrode)

73   reproducibility becomes a concern.

74   There has been an effort over the past few years to create reusable hybrid devices with

75   conventional lithographic fabrication techniques. This effort includes reusable, hybrid

76   devices fabricated from polystyrene[13-15] or polyester[16] as well as utilization of epoxy to

77   embed electrodes.[17, 18] It has been shown that electrodes can be integrated in several of

78   these substrates,[13, 14, 17, 18] with polishable electrodes. While more rugged and reusable

79   than their polymer counterparts, the ease of customization and integration of these hybrid

80   devices with commercial parts is still limited. For example, the PDMS layer of such a hybrid

81   device can be integrated with a reusable epoxy or polystyrene base,[13] but the rigid,

82   polystyrene layer still must be removed, cleaned, aligned, and resealed prior to use for

83   additional experiments. The need to realign and reassemble devices contributes to reduced

84   precision for biological studies requiring replicate studies and controls.

85   To date, in the chemical sciences, 3D printed devices have been utilized mostly for

86   organic synthesis reactionware.[19-23] Applications in the biomedical fields include tissue

87   scaffold development, [24-26] but the potential for the technology to significantly impact the

88   field of microfluidics is high.[27, 28] We recently reported on the use of 3D printers to fabricate

89   fluidic devices, with the printing of channels, integration of tubing to the device, and

90   incorporation of a membrane above the channel in order to study drug transport and

91   affect.[29] Other 3D printed devices have been utilized by the Spence laboratory to

92   quantitatively investigate the properties of stored red blood cells for transfusion

93   medicine.[30] The latter device utilized a circulating pumping scheme that could be

94   disconnected prior to placement of the entire printed device into a commercial plate reader

95   for quantitation of released cellular metabolites.   In both of the reported studies, detection

96   schemes were either optical or based on off-device mass spectrometric determinations.

97   To date, integrated electrochemical detection schemes have not been reported with 3D

98   printed devices. Here, we show that the integration of removable, reusable electrodes with

99   3D printed devices can be achieved by fabricating electrodes inside a commercial fitting

100   whose dimensions are well documented and that can be easily transferred among labs. The

101   use of commercially available components having defined and standardized dimensions is

102   imperative because it enables the fluidic device to be printed to accommodate such

103   commercially defined parts.   Importantly, the threaded functionality of the electrodes

104   allows for ease of removal, repolishing, and reuse should the electrode become

105   compromised, a significant advance for electrochemical detection in fluidic devices. For

106   example, metal electrodes fabricated inside micron-sized polymer channels using

107   deposition techniques can be used with biological samples, but cannot be reused. We

108   present two 3D printed devices, one capable of housing electrodes (both working and

109   reference) for electrochemical detection in 500 μm wide channels, and the other capable of

110   analyte   collection   while   simultaneously   measuring   oxygen   concentration

111   chronoamperometrically. The latter device was used to correlate the effect of oxygen

112   tension on the release of ATP from red blood cells (RBCs) flowing through the channels of a

113   printed device. Collectively, these studies demonstrate that different electrode materials

114   can easily be introduced to the device. In fact, here, the limiting step to perform replicate

115   experiments was the electrode and/or sample preparation rather than quality control of

116   the microfluidic platform. Unlike traditional microfluidic devices, the technology can be

117   shared via .STL files to promote standardization within the field.

118   **Experimental**

119   *Materials*

120   The following chemicals and materials were used as received: 0.5 mm gold wire, 0. 5 mm

121   silver wire, firefly lantern extract, catechol, dopamine hydrochloride, chloroplatinic acid

122   hydrate, lead (II) acetate trihydrate, Hanks' balanced salt solution (HBSS), TES (Trizma

123   acetate, ethylenediaminetetraacetic acid (EDTA), sucrose) buffer, and potassium nitrate

124   (Sigma Aldrich, St. Louis, MO); Armstrong C-7 resin, Activator A and E (Ellsworth

125   Adhesives, Germantown, WI); silver conductive epoxy (MG Chemicals, Burlington, ON,

126   Canada); J-B Kwik (J-B Weld Co., Sulphur Springs, TX); 250 and 500 µm platinum wire, 2

127   mm palladium wire, and 1 mm glassy carbon rod (Alfa Aesar, Ward Hill, MA); soldering

128   wire and heat shrink tubes (Radio Shack); isopropanol and acetone (Fisher Scientific,

129   Springfield, NJ); colloidal silver (Ted Pella, Redding, CA); electrode polishing pads (CH

130   Instruments, Austin, TX; Allied High Tech Products, Inc., Rancho Dominguez, CA); nitric

131   oxide (NO) tank (99.5%) (Airgas Inc., Radnor, PA); polyetheretherketone (PEEK) fitting

132   nuts (P-131: 1/8" outer diameter (o.d.) tubing, P-137: 3/16" o.d. tubing), one-piece finger

133   tight fittings for 1/16" o.d. tubing (IDEX Health & Science, Oak Harbor, WA); Nafion (5%

134   w/w Nafion, Ion Power Inc., New Castle, DE or Sigma Aldrich, St. Louis, MO).

135

136   *3D Printed Device Fabrication*

137   Devices were designed in Autodesk Inventor Professional 2014 Student Edition. The part

138   file was converted to an .STL file and was subsequently submitted for printing to the

139 Department of Electrical and Computer Engineering at Michigan State University. The

140 printer used was an Objet Connex 350 Multi-material 3D printer with VeroClear, which is a

141 proprietary acrylate-based polymer material. The support material was cleared with

142 compressed air. Further clearing of the support material was accomplished using

143 polyimide-coated capillaries, compressed nitrogen, and sonication.

144

145 *Electrode Fabrication*

146 For the fabrication of epoxy-embedded electrodes in flangeless fitting nuts, electrode

147 materials (250 and 500 μm platinum wire for platinum black; 1 mm glassy carbon rod and

148 2 mm palladium wire for glassy carbon) were cut to desired length (5 mm) and affixed,

149 either by soldering or connection with colloidal silver, to a copper extending wire to

150 provide the electrical connection. Heat shrink tubing was used to insulate the connection.

151 The electrodes were inserted into the 1/8" o.d. PEEK fitting nut with serial alignment, such

152 that sample first flowed over the working electrode. Following the assembly of the fitting

153 nut and electrode, a thoroughly mixed combination of Armstrong C-7 adhesive (resin) and

154 Armstrong Activator A was poured into the fitting and left to cure overnight. Later, the

155 epoxy-filled fitting nut containing the electrodes was polished by wet polishing. For the

156 fabrication of epoxy-embedded electrodes for oxygen detection, electrode materials (0.5

157 mm gold and 0.5 mm silver wire) were cut to desired length (5 mm) and affixed with

158 conductive epoxy to a copper extending wire to provide the electrical connection. The

159 connection was reinforced with J-B Kwik Weld. The electrodes were secured into the 3/16"

160 o.d. PEEK fitting nut, and a thoroughly mixed combination of Armstrong C-7 adhesive

161 (resin) and Armstrong Activator E was poured into the fitting and was left to cure

162   overnight. The fabricated electrode was wet polished with P1000 grit sandpaper (3M, St.

163   Paul, MN) to expose the electrodes and was subsequently polished with 0.05 μm alumina

164   powder (CH Instruments).

165   *Electrode Modification*

166   For exclusion studies, Nafion coatings over the glassy carbon electrodes used for dopamine

167   detection were prepared by physical deposition with 1 μL of a 0.05% Nafion solution

168   (prepared in isopropyl alcohol from a 5% solution of commercially available Nafion) that

169   was left to dry on the electrodes overnight. For the preparation of platinum black

170   electrodes (250 μm Pt), the PEEK nut fitting containing the electrode and a Ag/AgCl

171   reference were immersed in a 10 mL beaker filled with 3.5% chloroplatinic acid (w/v) and

172   0.005% lead (II) acetate trihydrate. Electrode plating was achieved by cycling the potential

173   from +0.60 to 0.35 V (vs. Ag/AgCl) at a scan rate of 20 mV/s (1 scan).

174   The electrodes used for oxygen detection were polished before each use with 0.05 μm

175   alumina powder, sonicated for 5-10 minutes, washed with deionized water, and placed in a

176   75 °C oven to dry for 10-15 minutes. After drying and cooling, the silver electrode was

177   coated with AgCl using 3 M KCl (Fisher Scientific, Pittsburgh, PA), a 9 V battery with leads,

178   and another Ag wire. After coating with AgCl, the electrodes were washed with deionized

179   water and dried again. A Nafion coating was applied by dipping the electrodes into a 2.5%

180   (for O_2 detection) w/w solution of Nafion diluted with isopropyl alcohol (prepared from a

181   5% w/w Nafion). The electrodes were dipped into the 2.5% Nafion solution and held for

182   approximately 10 seconds until the electrodes were completely covered by solution. The

183   electrodes were then allowed to dry on the bench top until ready for use in the printed

184   device.

185

186 *Flow Injection Analysis with a 3D Printed Device*

187 The setup for flow injection analysis using PDMS devices and electrochemical detection has

188 been previously reported.[6, 31, 32] In this study, a similar approach was taken, with the 3D

189 printed devices serving as the fluidic platform. In studies for Pt-black and glassy carbon

190 electrode characterization, the device used contained a straight channel (500 μm width,

191 500 μm height, and 3 cm length). For characterization studies with the straight channel, the

192 appropriate buffer was continuously pumped at 8.0 μL/min into the channel *via* a 500 μL

193 syringe (SGE Analytical Science, Austin, TX) and a syringe pump (Harvard 11 Plus, Harvard

194 Apparatus, Holliston, MA). The syringe was connected to 150 μm i.d. capillary tubing using

195 a finger tight PEEK fitting and a luer adapter (Upchurch Scientific, Oak Harbor, WA). The

196 same connectors and a 150 μm i.d. capillary fitted with a 350 μm o.d. PEEK tubing sleeve

197 (Idex) were used to transition from a 4-port rotary injection valve (VICI Rotor, Valco

198 Instruments, Houston, TX) to the device. The 4-port injection valve enabled reproducible

199 200 nL injections to the printed flow channel. Amperometric detection was performed

200 with a 2-electrode system driven by potentiostat. The working electrode was glassy

201 carbon, platinum, or platinum/platinum-black. Either palladium or platinum were used as

202 the pseudo-reference electrode; both working and pseudo-reference electrodes were

203 epoxy-embedded in a PEEK nut and fitted with the threads aligned with the 3D printed

204 threaded port (i.e., not physically tapped) on the device. The PEEK nut was turned

205 clockwise for tightening. A working electrode potential of +0.9 V (vs. Pt or Pd) was utilized

206 for characterization studies using Pt, Pt-black, or glassy carbon.

207

208   HBSS and TES (pH 7.4) buffers were used, respectively, for characterization studies with

209   NO and dopamine. For flow studies with NO, an NO standard stock solution (1.9 mM) was

210   prepared by deoxygenating HBSS with Ar for 30 minutes, then saturating the solution with

211   NO gas (99.5%) for 30 minutes.[33] The NO gas was purified before use by passing it through

212   a column packed with KOH pellets to remove trace NO degradation products. Individual

213   samples were made in deoxygenated volumetric flasks (sealed with suba seal) and

214   deoxygenated HBSS.

215

216   *Oxygen Standard Solutions*

217   A calculation of oxygen standard concentrations was performed starting with Henry's Law,

218   where the partial pressure of oxygen was assumed to be 0.20946 atm, and Henry's

219   constant for oxygen was 769.23 atm/M. Air-purged and argon-purged solutions were

220   prepared by sparging compressed air or argon into HBSS in a 100 mL round bottom flask

221   for at least 30 minutes. Oxygen standards were prepared by mixing measured volumes of

222   air-purged HBSS (saturated) and argon-purged HBSS (deoxygenated) in a 500 μL syringe.

223   The oxygen concentrations of both air- and argon-purged buffers were confirmed with a

224   commercial oxygen probe (Symphony SP70D, VWR). The argon-purged and air-purged

225   solution oxygen concentrations did not differ significantly from the calculated values using

226   Henry's constant. To prepare oxygen standard solutions with RBCs, the two argon-purged

227   and air-purged buffers were added to the syringe first, and then packed RBCs were added

228   to the syringe at an appropriate volume to create a 7% solution of RBCs.

229

230   *RBC Purification*

231   Blood collection procedures were approved by the Biomedical, Health Sciences

232   Institutional Review Board (BIRB) at Michigan State University. Human whole blood was

233   obtained by venipuncture from informed, consenting donors and was collected into 10 mL

234   Vacutainer tubes coated with lithium heparin (BD Biosciences, San Jose, CA) to prevent

235   coagulation. RBCs were initially separated from the plasma and buffy coat by centrifuging

236   the whole blood at 500 g at 25°C for 10 minutes. The supernatant and buffy coat were

237   removed by aspiration, and the RBCs were washed with HBSS and centrifuged again at 500

238   g for 10 minutes. This process was repeated twice more for a total of three washes with

239   HBSS. The hematocrit of the purified RBCs was determined with a StatSpin CritSpin micro-

240   hematocrit centrifuge (Iris Sample Processing, Inc., Westwood, MA).

241

242   *Chronoamperometric Oxygen Measurements*

243   Electrochemical measurements of oxygen were performed using a commercially available

244   potentiostat (CH Instruments). The 3D printed device hosting the electrodes used for

245   oxygen detection had a channel measuring 7 mm in length, 3 mm in width, and 0.5 mm in

246   height. The device contained a threaded electrode port for the gold and Ag/AgCl electrode.

247   The 3/16" nut housing the electrodes was screwed into the threaded port, and the

248   electrodes were attached to the potentiostat via leads. Flow of oxygen standards with or

249   without 7% RBCs (6 μL/min) from 500 μL syringes was controlled using a syringe pump

250   (Harvard). Samples were interfaced to the device through segments of 50 μm i.d. capillary

251   tubing and the same finger tight fittings and luer locks described above. Unless otherwise

252   specified, parameters for chronoamperometric measurement of oxygen are as follows:

253   Initial V: 0 V; High V: 0 V; Low V: -1 V; Initial step polarity: negative; Number of steps: 2;

254   Pulse width: 1 s; Sample interval: 0.001 s; Quiet time: 2 s; Sensitivity (A/V): 1×10^{-5}.

255   Calibration curves were generated using current values at 0.3 seconds from the

256   chronoamperograms.

257

258   *ATP Detection*

259   Transwell membrane inserts (polyester, 0.4 μm pores, Corning, Corning, NY) were inserted

260   into the well ports in the 3D-printed device. The well inserts were filled with 200 μL of

261   HBSS, and stable RBC flow (6 μL/min) was established, i.e., no air bubbles. The wells were

262   covered with a wet Kim-wipe to minimize evaporation from wells, and the 7% RBCs were

263   allowed to flow for 20 minutes. Next, the HBSS in the wells was collected into 600 μL posi-

264   click tubes (Denville Scientific, South Plainfield, NJ), which were stored on ice until all

265   samples were pumped through the device. 50 μL of each sample were plated in triplicate

266   on a 96-well plate. A luciferin luciferase mixture was prepared by adding 2 mg D-Luciferin

267   (GoldBio, St. Louis, MO) to 5 mL of distilled, deionized water (DDW). This 5 mL mixture was

268   added to a vial of firefly lantern extract, which was shaken until solids were dissolved. The

269   mixture was divided into 100 μL aliquots and frozen for storage. Aliquots were thawed and

270   diluted 1:1 with HBSS on the day of the experiment. To measure the RBC-derived ATP in

271   the transwell inserts, 50 μL of the luciferin luciferase mixture were pipetted with a

272   multichannel pipette into the wells, and the resulting chemiluminescence was immediately

273   read with a commercial plate reader (SpectraMax M4, Molecular Devices, Sunnyvale, CA).

274
275   *Imaging*

276   Color images, with the exception of the image shown in Figure 1C and 6B, were captured

277   with an upright Olympus, BX51 microscope equipped with an Infinity3 camera (Hitschfel

278   Instruments, Inc). Black and white non-fluorescent images were obtained from a

279   stereoscope (Olympus SXZ12) operating in bright field mode using a Sony 3CCD color

280   camera (Leeds Precision Instruments, Minneapolis, MN). The black and white non-

281   fluorescent images in Figures 4 and 5 were captured with an upright fluorescence

282   microscope using the bright field setting with a CCD camera (Olympus MVX10).

283

284   **Results and Discussion**

285   *Standardization of Devices Between Labs*

286   The use of parts with defined dimensions was essential in that the fluidic device was

287   fabricated to accommodate the commercial part. That is, the choice of electrode housing

288   (PEEK nuts) for these studies, in part, drove the 3D device design. It was important that the

289   electrode housings had fixed outer diameters, while the interior diameters could vary,

290   depending on the size of electrodes to be incorporated. Secondly, it was important that the

291   electrode housings have threads so they could be easily removable. More importantly, the

292   threads were of the same standard type, i.e., 5/16-24, for the two types utilized in this

293   study, allowing the electrodes to be used interchangeably between devices, if necessary.

294   These properties of the electrode housings allowed printing of an electrode port in both 3D

295   devices that could be used with various models of nuts because both parts had the same

296   outer diameter and threading. The only difference between the housings was the internal

297   diameter; this difference enabled the authors take liberty in the choice of electrode wire

298   diameters and in the electrode alignment with channels, particularly in the 500 μm wide

299   channel device. The nut used for fabrication of glassy carbon and Pt-black electrodes was

300   the P-131 model, while the P-137 model was used for the gold and Ag/AgCl electrode. This

301   standardization of the electrode port allowed for the electrodes of varying materials to be

302   made in different labs. The microfluidic device used for characterization studies for glassy

303   carbon and Pt-black was printed at Michigan State University and was shipped to the

304   Martin lab at Saint Louis University for collaboration. The fact that a device can be made in

305   one lab and utilized in another demonstrates the transferability when using 3D printed

306   devices. Although the transferability of the .STL file between academic laboratories is

307   expected to ease fabrication requirements, the variety of printable materials and printing

308   techniques are two factors that will create challenges for researchers. These two factors

309   can impact the dimensions and ultimately the functionality of a printed device or part. This

310   is due to the variation in resolution and in printer types (stereolithography, fused

311   deposition modeling, etc.) and also in the desired materials' physical properties.

312

313   *Integration with Microfluidic Channels*

314   Devices were designed and modified in Autodesk software using the dimensions of the

315   above-mentioned, commercially available fittings. For the devices presented herein,

316   dimensions in the part files were set and iteratively corrected using both part dimensions

317   provided by the supplier and also by manually measuring with calipers. Devices required

318   multiple iterations to achieve acceptable contact points for inlets/outlets, well inserts and

319   electrode ports. It is also worth mentioning that if a different material for the device is

320   desired, this iterative process must be repeated for printing with a different material. This

321   is due to differences in material properties that result from changes in material

322   composition as well as the printer type. For example, a device printed in one material will

323   not have exactly the same dimensions as the same device printed in another material, even

324 with the same printer, because of changes in the material properties. The dimension

325 precision, which is termed tolerance by the 3D printing community, is estimated to be on

326 the order of tenths of millimeters. However, this has yet to be investigated thoroughly for

327 the devices reported here.

328 Electrode alignment in the 500 μm channel device was achieved by sanding the PEEK nut

329 to remove threading until the electrodes were flush with the channel when the nut was

330 fully tightened, ensuring the same alignment each time the electrode was used. While this

331 method worked well for these studies, it is anticipated that in future fabrication, alignment

332 of the electrodes with channels can be addressed in the design process with the CAD

333 program (by integrating the electrode nut and device together in the part file to check

334 alignment) or in the fabrication step. For example, fabrication of working and

335 counter/reference wires in separate, smaller diameter 3D printed fittings that are

336 geometrically directly opposed in the channel would not only ease fabrication

337 requirements, but also allow for better control over electrode placement. Separate

338 alignment of electrodes could be spatially more practical for experimental design, but more

339 importantly it could also minimize the dead volume associated with connections to the

340 device. The dead volume in these two devices was not observed to interfere significantly

341 with the electrochemical measurements. The calculated dead volume for the inlet, obtained

342 by using measured distances with calipers, was estimated to be about 0.13 μL, assuming

343 the area between the fitting end and the beginning of the channel was conical in shape due

344 to mismatch between the fitting and conical inlet. This volume constitutes approximately

345 3.3% of the total volume of the 500 μm device (3.9 μL). It is difficult to estimate the dead

346 volume in the electrode fitting and in the membrane area by measuring with calipers due to

347 visual obstruction by the fitting and membrane. However, no deleterious effects, such as

348 band broadening or peak splitting, were observed due to dead volume in the flow injection

349 analysis or chronoamperometric data.

350 Channel widths in the presented devices are either 0.5 mm or 3 mm. Devices with 250 µm

351 and 100 µm wide channels were printed, but fluid flow was obstructed by the un-removed

352 support material that was present in the channel post-print. Currently, removal of support

353 material is accomplished using compressed air, sonication, and scraping. This limits the

354 use of sub-500 µm in width channels for this study, as it becomes difficult to clear support

355 material out of smaller dimension channels. However, it is anticipated that as polishing

356 techniques, both physical and chemical in nature, for these cured acrylate-based materials

357 improve, sub 500 µm features will become possible to fabricate consistently.

358

359 *Fabrication and Characterization of Glassy Carbon and Pt-black*

360 For the first time, electrode materials were integrated with a 3D printed microfluidic

361 device (500 µm channel width) to enable electrochemical detection of electroactive species,

362 in this case dopamine and NO (Figure 1). The same physical device was used with both

363 glassy carbon and Pt-black electrodes. This was possible because the electrode housing was

364 a standard 5/16-24 threaded fitting, which allows for any fitting with the appropriate

365 diameter and threading to be integrated with the device. Parts A & B in Figure 1 show the

366 Autodesk rendering of the device, where threads and channel can be visualized in three

367 dimensions. This visualized file is termed the part file and is the precursor to the .STL file

368 submitted for printing. Figure 1C is a micrograph of the threaded epoxy-embedded

369 electrodes aligned in the center of the 500 µm channel. Part D in Figure 1 shows the

370   assembled device with commercial fittings, electrode, and electrode leads. This setup is

371   interfaced with a syringe pump and with a 4-port injection valve with a loop volume of 250

372   μL.

373   A major application of microfluidic-based electrochemical detection is monitoring

374   neurotransmitters; therefore, the integration of commonly used carbon electrodes for

375   catecholamine detection was demonstrated. Specifically in these studies, a glassy carbon

376   working electrode (1 mm diameter) was utilized to detect dopamine. When utilized with

377   flow injection analysis, the embedded 1 mm glassy carbon electrode could measure a 500

378   nM limit of detection (LOD) for dopamine in the 500 μm channel device with linear

379   response (R^2 = 0.99) for a wide range of concentrations (25-500 μM).

380   Electrode modifications, such as a coating with a perm-selective membrane like Nafion to

381   selectively permit neutral or positive small molecules to the electrode, are widely used to

382   make electrodes more selective toward an electroactive species.[34, 35] To investigate the use

383   of Nafion for selectivity, the glassy carbon electrode was coated with a 0.05% Nafion

384   solution and was used for flow injection analysis. As can be seen in Figure 2, significant

385   exclusion of 100 μM nitrite was achieved with the Nafion-coated electrode (average peak

386   height = 0.31 ± 0.02 nA, n = 3) when compared to signal obtained from equimolar injections

387   of dopamine over the same electrode (average peak height = 1.83 ± 0.06 nA, n = 3, see

388   Figure 2, panel B) and nitrite over an unmodified electrode (average peak height = 2.80 ±

389   0.02 nA).

390   Platinum electrodes are commonly used for NO detection[36] and can be made more sensitive

391   for NO with the use of platinized electrodes.[37] In the platinization process, a chloroplatinic

392   acid solution, which contains a small amount of lead acetate, is used to electrochemically

393   deposit black particles of platinum onto the platinum working electrode. The optimal

394   deposition cycle to be used for NO detection in microfluidic devices has previously been

395   determined.[38] Figure 3 illustrates a bare 500 μm Pt electrode (used as the pseudo-

396   reference) and the Pt-black surface modification on the 250 μm platinum working

397   electrode. To demonstrate the signal enhancement resulting from the Pt-black deposition

398   on platinum, repeated injections of a 190 μM NO solution were analyzed with a bare Pt or

399   Pt-black electrode. As shown in Figure 3, a nearly 7-fold signal increase was observed for

400   NO detection with the Pt-black modified platinum electrode (average peak height = 3.61 ±

401   0.02 nA, n = 3) relative to a bare platinum electrode (average peak height = 0.54 ± 0.06 nA,

402   n = 3). Others have previously reported similar values in signal enhancement (8-13 times

403   signal amplification) when using Pt-black electrodes for NO detection in studies not

404   involving microfluidic devices.[37] When using flow injection analysis and standards derived

405   from NO gas, the 250 μm platinum electrode modified with Pt-black exhibited a

406   reproducible response (RSD = 4.2%, n=12) (average peak height = 2.63 ± 0.11 nA, n=12).

407   An NO calibration curve for this electrode demonstrated a linear correlation (R^2 = 0.99)

408   over a wide range of concentrations (7.6 - 190 μM). The LOD for NO on this Pt-black

409   electrode was 1 μM.

410   *Fabrication and Integration of Gold and Ag/AgCl Electrodes for Oxygen Detection in*

411   *Biological Samples*

412   Clark-type electrodes, using platinum,[39, 40] silver[41, 42] or gold[43-45] working electrodes, are

413   commonly used for measuring dissolved oxygen in biological samples. To determine if

414   Nafion-coated gold and Ag/AgCl electrodes (Figure 4A), fabricated and modified as

415   described above, were suitable for oxygen detection in 7% RBCs in the 3D printed device,

416   oxygen standards in the presence and absence of 7% RBCs were measured (Figure 4B). The

417   device for this characterization contained a channel 3 mm in width, 0.5 mm in height and a

418   threaded inlet, outlet, and electrode port. The 3 mm wide channel dimension was chosen to

419   accommodate both the 0.5 mm electrodes as well as the transwell membrane inserts for

420   the studies described below. After confirmation that the electrode response had a linear

421   relationship with oxygen concentration (Figure 4B), the device part file was modified to

422   include two wells to house membrane inserts and was resubmitted for printing, resulting

423   in the device displayed in Figure 5. This modification step took significantly less time

424   (hours) than traditional lithographic techniques, which would require creation of a new

425   master (at least 1 day). Three electrodes were fabricated for oxygen detection and were

426   used to collect the chronoamperometric data. The average signal from the three electrodes

427   for an 8.74 ppm oxygen standard with 7% RBCs was 0.83 µA, and the standard deviation

428   was 0.10 µA, resulting in an RSD of 12%.

429   *Electrochemical Detection of Oxygen in a Stream of Flowing Hypoxic RBCs Using a 3D Printed*

430   *Device*

431   The electrochemical and fluorescence detection of biologically relevant analytes in

432   microfluidic devices has been previously reported.[46-48] Here, we demonstrate the

433   amenability of a rigid, 3D printed device for electrochemical detection of oxygen in a

434   stream of flowing hypoxic RBCs, while simultaneously collecting the ATP released from

435   these cells in a transwell insert incorporated into the device. This device (Figures 5 and 6)

436   facilitated measurement of these two analytes by including a threaded port (5/16-24

437   threading) for the removable Nafion-coated gold and Ag/AgCl electrode and two wells to

438   house   membrane   inserts   (0.4   µm   pores).   The   electrode   was   used   to

439   chronoamperometrically measure the oxygen tension in a flowing stream of RBCs, while

440   the membrane inserts were used to simultaneously collect ATP release for off device

441   chemiluminescence detection, as described above. ATP release from flowing normoxic

442   RBCs (8.22 $\pm$ 0.60 ppm oxygen) and from flowing hypoxic RBCs (4.76 $\pm$ 0.53 ppm oxygen)

443   was compared. Raw chemiluminescence intensity values from triplicate normoxic and

444   hypoxic samples were averaged, and the values were normalized to the normoxic sample

445   values. The normalized data are presented in Figure 6C. The hypoxic RBC samples released

446   on average 2.37 $\pm$ 0.37 times more ATP than the normoxic RBC samples.

447   Previous work from the Spence group[49, 50] has focused on measuring metabolite release

448   from hypoxic RBCs to determine the underlying mechanism and biological importance of

449   hypoxia-induced vasodilation. An attractive property of the acrylate-based printing

450   material is its low permeability to oxygen. In the above oxygen measurements, it was

451   desired that the device material not be as permeable to oxygen as compared to PDMS in

452   order to minimize the background signal at the Nafion-coated electrodes. A rigid, 3D

453   printed device that can be sterilized using traditional methods (rinsing with ethanol),

454   reused as desired, and coupled with various electrode materials and well inserts that are

455   amenable to cell culture, is an attractive platform for more complex biological studies.

456   **Conclusions**

457   3D printing is a fabrication method that can be used to print rigid, reusable fluidic devices.

458   In this paper, we were able to show that a variety of electrode materials (carbon, platinum,

459   gold, silver) for a wide range of applications (neurotransmitter detection, NO detection,

460   measuring oxygen tension in a stream of red blood cells) can be easily integrated into these

461   devices along with other functionalities such as fluidic interconnects and membrane inserts

462   to enable signaling molecule detection (ATP via chemiluminescence). Because of the

463   dimensional control that computer-aided design (CAD) programs allow, these devices can

464   be easily integrated with commercially available parts whose dimensions are known or can

465   be measured. This enables a module-like approach to experimental design, allowing a

466   researcher to fabricate a multicomponent device, troubleshoot any problems, modify or

467   add to the part file, and reprint for continued study – all on a similar or faster time scale

468   than with photo- and soft lithographic techniques. Unlike the physical format of soft

469   lithographic masters, the part files for 3D printing are standardized, i.e., the part can be

470   exchanged with and transferred to any lab that has access to a CAD program and 3D

471   printer. Importantly, the electrode fitting is removable and reusable, a significant

472   improvement over the traditional one-time-use evaporation/deposition-based metal

473   electrodes. This technology has the potential to not only change the way that researchers

474   approach collaboration but also our perceived limitations of experimental designs,

475   particularly in biological studies where spatial control of samples or cells is critical.

476

477

478

483

484   **References**

485   1.   R. S. Martin, A. J. Gawron, S. M. Lunte and C. S. Henry, *Anal Chem*, 2000, 72, 3196-
486   3202.
487   2.   A. T. Woolley, K. Lao, A. N. Glazer and R. A. Mathies, *Anal. Chem.*, 1998, 70, 684-688.
488   3.   J. A. Vickers and C. S. Henry, *Electrophoresis*, 2005, 26, 4641-4647.
489   4.   A. J. Gawron, R. S. Martin and S. M. Lunte, *Electrophoresis*, 2001, 22, 242-248.
490   5.   M. L. Kovarik, M. W. Li and R. S. Martin, *Electrophoresis*, 2005, 26, 202-210.
491   6.   M. L. Kovarik, N. J. Torrence, D. M. Spence and R. S. Martin, *Analyst*, 2004, 129, 400.
492   7.   P. J. Castle and P. W. Bohn, *Anal Chem*, 2004, 77, 243-249.
493   8.   A. L. Bowen and R. S. Martin, *Electrophoresis*, 2010, 31, 2534–2540.
494   9.   N. A. Lacher, S. M. Lunte and R. S. Martin, *Anal. Chem.*, 2004, 76, 2482-2491.
495   10.   C. Amatore, N. Da Mota, C. Lemmer, C. Pebay, C. Sella and L. Thouin, *Anal. Chem.*,
496   2008, 80, 9483-9490.
497   11.   D. P. Manica, Y. Mitsumori and A. G. Ewing, *Anal. Chem.*, 2003, 75, 4572-4577.
498   12.   A. S. Johnson, A. Selimovic and R. S. Martin, *Anal Bioanal Chem*, 2013, 405, 3013–
499   3020.
500   13.   A. S. Johnson, K. B. Anderson, S. T. Halpin, D. C. Kirkpatrick, D. M. Spence and R. S.
501   Martin, *Analyst*, 2013, 138, 129-136.
502   14.   K. B. Anderson, S. T. Halpin, A. S. Johnson, R. S. Martin and D. M. Spence, *Analyst*,
503   2013, 138, 137-143.
504   15.   M. R. Dusseiller, D. Schlaepfer, M. Koch, R. Kroschewski and M. Textor, *Biomaterials*,
505   2005, 26, 5917-5925.
506   16.   G. S. Fiorini, R. M. Lorenz, J. S. Kuo and D. T. Chiu, *Anal Chem*, 2004, 76, 4697-4704.
507   17.   A. S. Johnson, A. Selimovic and R. S. Martin, *Electrophoresis*, 2011, 32, 3121-3128.
508   18.   A. Selimovic, A. S. Johnson, I. Z. Kiss and R. S. Martin, *Electrophoresis*, 2011, 32, 822-
509   831.
510   19.   V. Dragone, V. Sans, M. H. Rosnes, P. J. Kitson and L. Cronin, *Beilstein Journal of*
511   *Organic Chemistry*, 2013, 9.
512   20.   P. J. Kitson, M. H. Rosnes, V. Sans, V. Dragone and L. Cronin, *Lab Chip*, 2012, 12, 3267-
513   3271.
514   21.   P. J. Kitson, M. D. Symes, V. Dragone and L. Cronin, *Chemical Science*, 2013, 4, 3099-
515   3103.
516   22.   J. S. Mathieson, M. H. Rosnes, V. Sans, P. J. Kitson and L. Cronin, *Beilstein Journal of*
517   *Nanotechnology*, 2013, 4, 285-291.
518   23.   M. D. Symes, P. J. Kitson, J. Yan, C. J. Richmond, G. J. T. Cooper, R. W. Bowman, T.
519   Vilbrandt and L. Cronin, *Nature Chemistry*, 2012, 4.
520   24.   E. N. Antonov, V. N. Bagratashvili, M. J. Whitaker, J. J. A. Barry, K. M. Shakesheff, A. N.
521   Konovalov, V. K. Popov and S. M. Howdle, *Advanced materials*, 2005, 17, 327-330.
522   25.   C. X. F. Lam, X. Mo, S.-H. Teoh and D. Hutmacher, *Materials Science and Engineering:*
523   *C*, 2002, 20, 49-56.
524   26.   M. Lee and B. M. Wu, *Methods in Molecular Biology*, 2012, 868, 257-267.
525   27.   B. C. Gross, J. L. Erkal, S. Y. Lockwood, C. Chen and D. M. Spence, *Anal Chem*, 2014,
526   140116094947007.
527   28.   A. Waldbaur, H. Rapp, K. Länge and B. E. Rapp, *Anal Methods-Uk*, 2011, 3, 2681-2716.

528 29. K. B. Anderson, L. S.Y., R. S. Martin and D. M. Spence, *Anal Chem*, 2013, 85, 5622-
529   5626.
530 30. C. Chen, Y. Wang, S. Y. Lockwood and D. M. Spence, *Analyst (Cambridge, United*
531   *Kingdom)*, 2014, (In Revision).
532 31. N. G. Batz and R. S. Martin, *Analyst*, 2009, 134, 372.
533 32. M. Hulvey and R. Martin, *Chem. Educator*, 2004, 9, 1-7.
534 33. J. H. Shin, B. J. Privett, J. M. Kita, R. M. Wightman and M. H. Schoenfisch, *Anal Chem*,
535   2008, 80, 6850-6859.
536 34. E. W. Kristensen, W. G. Kuhr and R. M. Wightman, *Anal Chem*, 1987, 59, 1752-1757.
537 35. J. B. Zimmerman and R. M. Wightman, *Anal Chem*, 1991, 63, 24-28.
538 36. K. Shibuki, *Neuroscience Research*, 1990, 9, 69-76.
539 37. Y. Lee, B. K. Oh and M. E. Meyerhoff, *Anal Chem*, 2003, 76, 536-544.
540 38. A. Selimovic and R. S. Martin, *Electrophoresis*, 2013, 34, 2092-2100.
541 39. G. Jobst, G. Urban, A. Jachimowicz, F. Kohl, O. Tilado, I. Lettenbichler and G. Nauer,
542   *Biosensors and Bioelectronics*, 1993, 8, 123-128.
543 40. L. C. Clark and C. Lyons, *Annals of the New York Academy of Sciences*, 1962, 102, 29-
544   45.
545 41. Z. Yang, S. Sasaki, I. Karube and H. Suzuki, *Anal Chim Acta*, 1997, 357, 41-49.
546 42. H. Suzuki, T. Hirakawa, I. Watanabe and Y. Kikuchi, *Anal Chim Acta*, 2001, 431, 249-
547   259.
548 43. G. J. Maclay, W. J. Buttner and J. R. Stetter, *IEEE Transactions on Electron Devices*,
549   1988, 35, 793-799.
550 44. G. W. McLaughlin, K. Braden, B. Franc and G. T. A. Kovacs, *Sensors and Actuators B:*
551   *Chemical*, 2002, 83, 138-148.
552 45. J.-H. Lee, T.-S. Lim, Y. Seo, P. L. Bishop and I. Papautsky, *Sensors and Actuators B:*
553   *Chemical*, 2007, 128, 179-185.
554 46. J. A. Lapos, D. P. Manica and A. G. Ewing, *Anal Chem*, 2002, 74, 3348-3353.
555 47. J. Wang and M. Pumera, *Anal Chem*, 2002, 74, 5919-5923.
556 48. K. Kisler, B. N. Kim, X. Liu, K. Berberian, Q. Fang, C. J. Mathai, S. Gangopadhyay, K. D.
557   Gillis and M. Lindau, *Journal of biomaterials and nanobiotechnology*, 2012, 3, 243.
558 49. S. T. Halpin and D. M. Spence, *Anal. Chem. (Washington, DC, U. S.)*, 2010, 82, 7492-
559   7497.
560 50. A. Faris and D. M. Spence, *Analyst*, 2008, 133, 678-682.
561
562

563

568   **Figure 1**
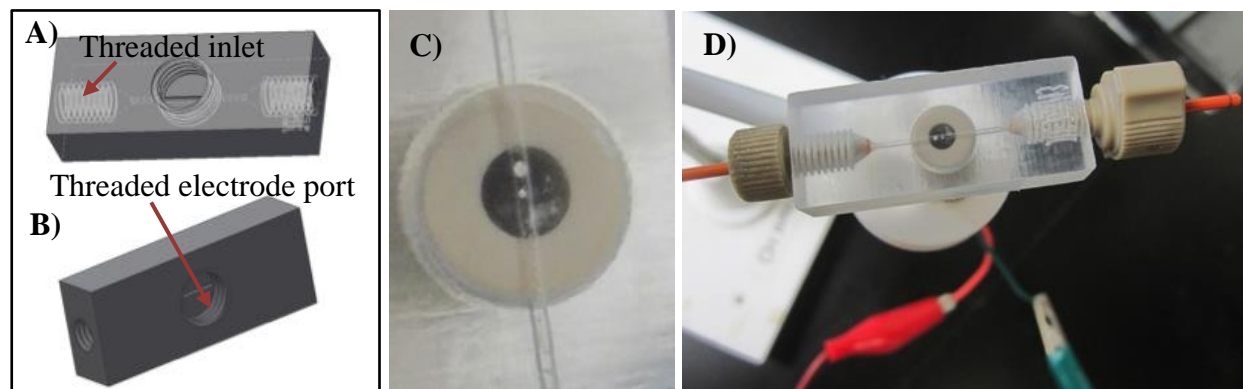
569

570   **Figure 1.** 3D device used for electrochemical detection. A-B) 3D renderings of the device in

571   Autodesk software; C-D) Printed 0.5 mm-wide channel device in VeroClear material. The Pt-

572   electrode is screwed into the electrode port, showing alignment of both Pt wires with the 0.5 mm

573   channel (panel C). In panel D, the device is shown with the Pt-electrode, electrode leads, and the

574   fittings used to integrate the device with a syringe pump.

575

576 **Figure 2**
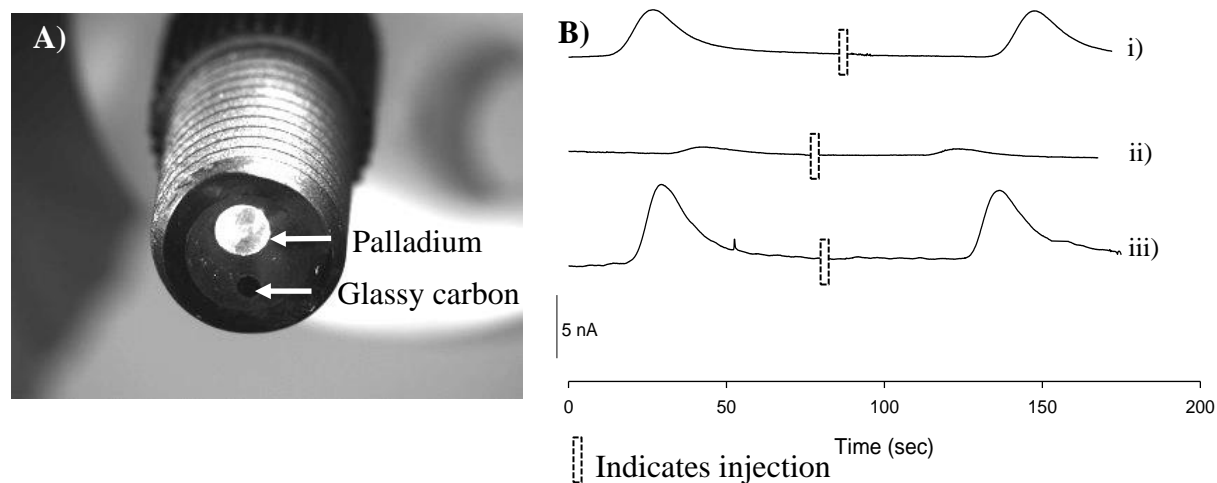
577

578 **Figure 2.** Glassy carbon working electrode for the detection of dopamine. A) Image showing the

579 flangeless fitting with a 2 mm palladium pseudo-reference and a 1 mm glassy carbon working

580 electrode; B) flow injection analysis to show selectivity of a Nafion-coated glassy carbon

581 electrode; i) Response for dopamine [100 μM] using the Nafion-coated glassy carbon electrode;

582 ii) Response for nitrite [100 μM] using the Nafion-coated glassy carbon electrode; iii) Response

583 for nitrite [100 μM] using a non-modified glassy carbon electrode.

584

585

586

587

588

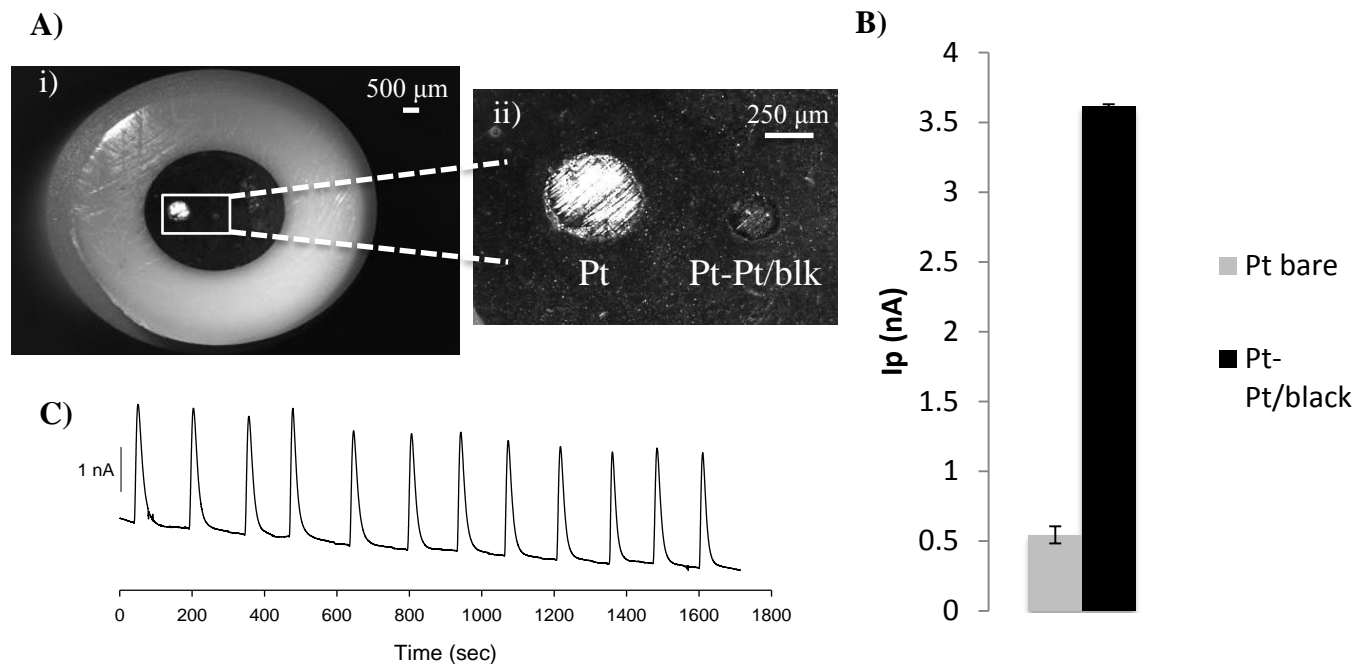589

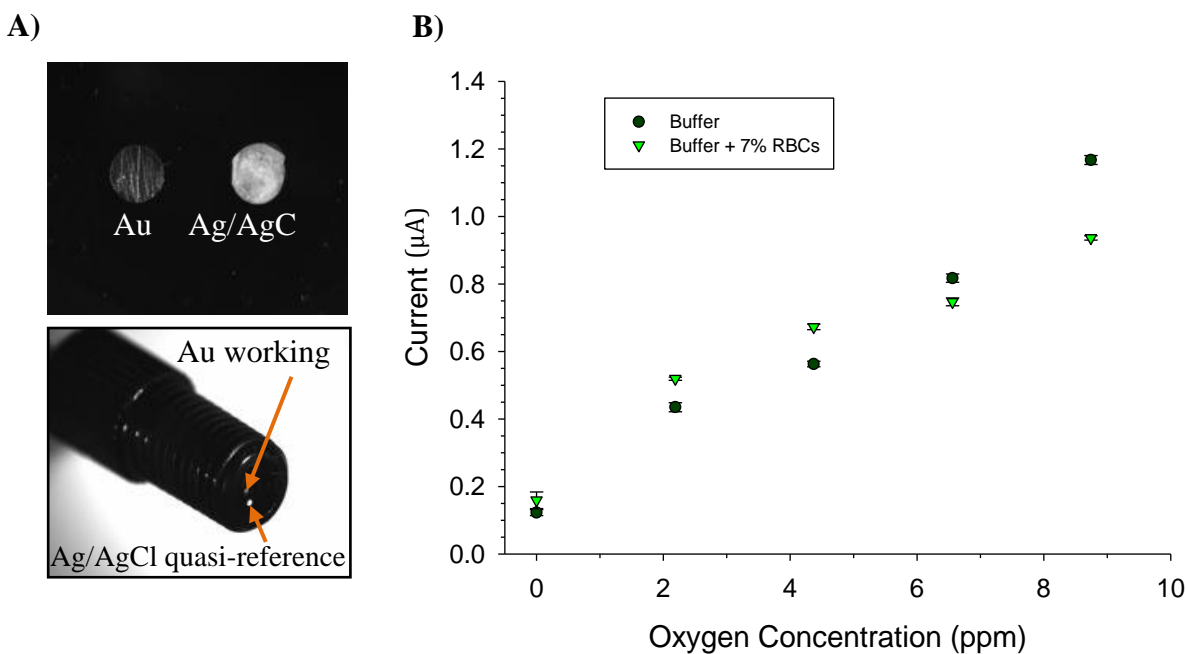590

591

592

593   **Figure 3**

594

595   **Figure 3**. Platinum electrodes for NO detection. A) i) Platinum pseudo-electrode (500 μm) and

596   platinum working electrode [250 μm] encapsulated with epoxy in a flangeless fitting; ii) Zoomed

597   micrograph of the platinum black modified platinum working electrode; B) Bar graph comparing

598   the signal for NO [190 μM] with a bare Pt electrode verses the Pt/Pt-black modified electrode; C)

599   Amperogram of reproducible 190 μM NO injections over the Pt/Pt-black electrode.

600

601

602

603

604

605

606

607

608   **Figure 4**

609

610   **Figure 4.** Measuring O_2 tension in a flowing stream of buffer (HBSS) and in HBSS with RBCs.

611   Measurements were made with a Nafion-coated gold electrode and Ag/AgCl quasi-reference

612   electrode. A) Micrographs of the electrode containing gold and silver wire secured with C-7

613   epoxy. In both micrographs, the silver wire is coated with AgCl; B) Calibration curve data for

614   oxygen standards in HBSS [$y=1.13 \times 10^{-7}x+1.26 \times 10^{-7}$; $R^2 = 0.98$] and in the presence of RBCs

615   [$y=8.15 \times 10^{-8}x+2.50 \times 10^{-7}$; $R^2 = 0.93$]. N = 1 electrode with triplicate measurement. Error =

616   standard deviation.
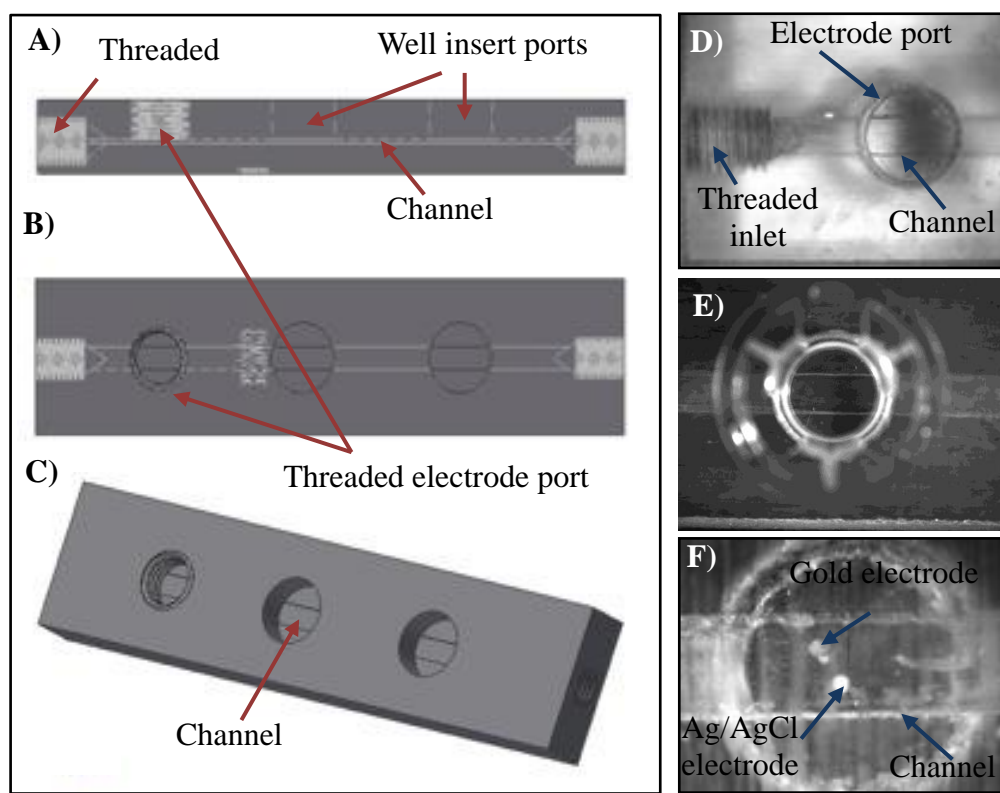
617

618

619

620

621

622

623   **Figure 5**

624

625   **Figure 5.** Fabrication of 3D device to measure oxygen and ATP from flowing RBCs. The left

626   side of the figure shows the rendering of the device in the Autodesk software. A) Side profile of

627   device detailing the threaded inlet, electrode port, and well insert ports; B) Top view of device;

628   C) Solid body view of device; D) 3D printed device in VeroClear material, detailing the inlet and

629   electrode port; E) Transwell membrane inserted into the device via the well insert port; F) 3D

630   printed device with electrode inserted fully into the port, showing the working and quasi-
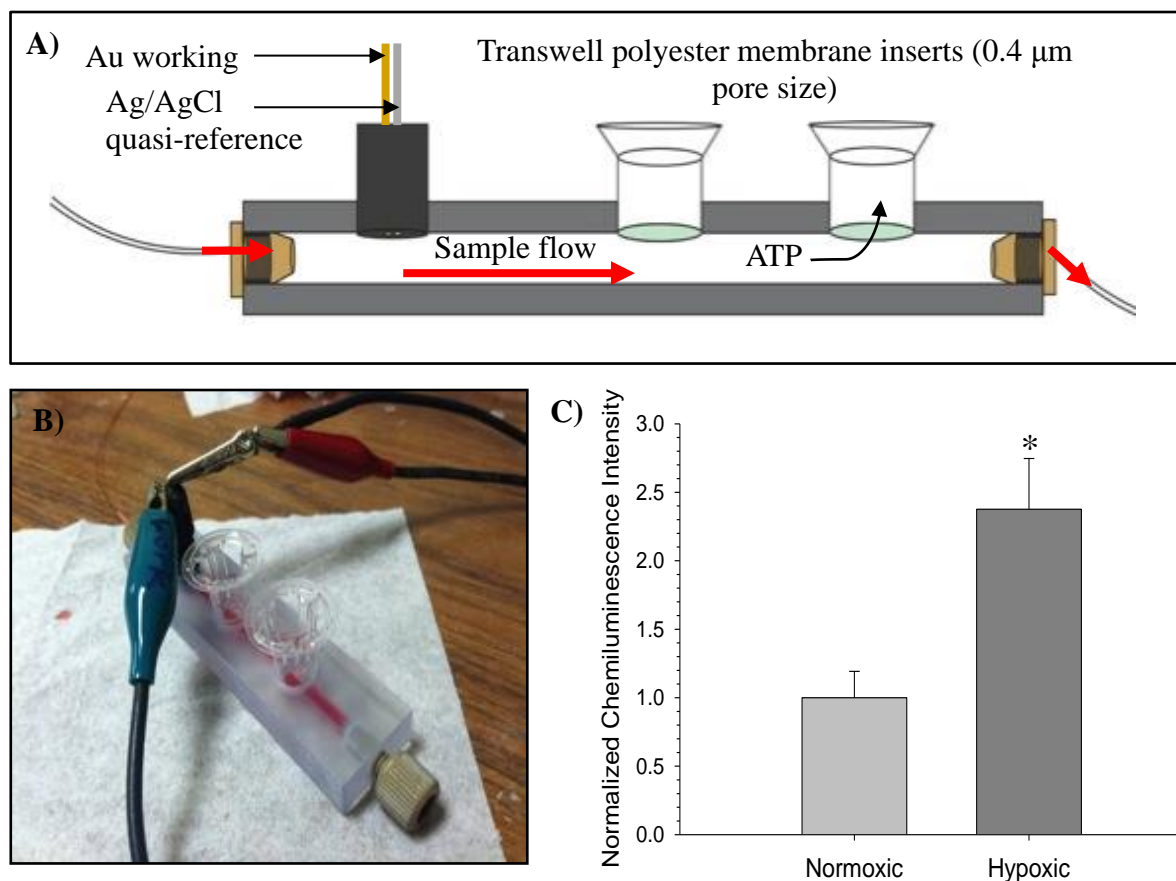
631   reference electrodes for oxygen sensing.

632

633

634

635

636   **Figure 6**

637

638   **Figure 6.** Fluidic device for correlation of oxygen tension and ATP release. A) Schematic of

639   device; B) Picture of the assembled device with RBCs being pumped through the system; C)

640   Comparison of RBC ATP release from a normoxic sample (8.22 ± 0.60 ppm oxygen) to a

641   moderately hypoxic sample (4.76 ± 0.53 ppm oxygen). N = 3 donors; error = s.e.m., * $p < 0.05$.

642